



Section 2. Fuel material selection and testing

Preparation of simulated inert matrix fuel with different powders by dry milling method

Y.-W. Lee ^{a,*}, H.S. Kim ^a, S.H. Kim ^a, C.Y. Joung ^a, S.H. Na ^a, G. Ledergerber ^b,
P. Heimgartner ^b, M. Pouchon ^b, M. Burghartz ^b

^a Korea Atomic Energy Research Institute, P.O. Box 105, Yuseong, Taejeon, South Korea

^b Paul Scherrer Institut, CH-5232 Villigen PSI, Switzerland

Abstract

Simulated zirconium oxide-based inert matrix fuel (IMF) has been prepared using cerium oxide replacing plutonium oxide, following the conventional pelletising route, in which an improved two-stage attrition mill was employed. Different methods have been applied for the powder preparation. In addition to powder mixing, nitrate solutions have been co-precipitated to bulk gel and to microspheres by the internal gelation process. The calcined porous microspheres were crushed in the attrition mill with a few passes. This co-precipitated powder was compared with three different mixtures of the four commercially available powders (ZrO_2 , Y_2O_3 , Er_2O_3 and CeO_2). Pellets of a standard size with relative densities higher than 90% TD and comparable grain and pore structures have been obtained. Based on these simulation tests both processes are found suitable for fabricating IMF pellets, which fulfil requirements of a commercial plutonium and uranium mixed oxide (MOX), where applicable. No intensive milling is required to form a solid solution in the sintering step for a $(Zr,Y,Er,Ce)O_{2-x}$ pellet. For the fabrication of plutonium-containing IMF, a similar behaviour can be expected. © 1999 Elsevier Science B.V. All rights reserved.

1. Introduction

The inventories of spent uranium fuel, and hence of plutonium generated by commercial nuclear power plants are continuously increasing. In Europe reprocessing of uranium-based fuel and MOX fabrication are industrial activities which will provide a competitive option for the back-end of the nuclear fuel cycle. Direct disposal of spent uranium fuel is under evaluation, but it raises the intrinsic problem of burying rather large volumes of relatively soluble material with a high content of fissionable isotopes. For the elimination of excess plutonium by transformation into an inaccessible waste form, zirconia-based inert matrix fuel (IMF) for energy production in light water reactors (LWR) has been proposed by PSI [1–4]. Zirconium oxide is stabilised by yttrium oxide in a single cubic phase and erbium is added as burnable poison for reactivity control. The

chopped claddings might also be seen as the source of zirconium for this matrix material, further reducing the waste volume and concentrating the radio-toxic materials.

Fabrication of IMF with a good dispersion of the fissile isotopes requires a homogenisation step in a dry route fabrication, whereas a wet co-precipitation of different constituents results in a homogeneous materials. The homogenisation in a dry route, however, can be easily obtained by powder milling through finely adjusting milling parameters and the subsequent sintering process.

In this paper, preparation of ZrO_2 -based IMF with plutonium has been simulated by use of CeO_2 , replacing PuO_2 , following the conventional dry pelletising route, in which various parameters of milling and sintering were taken as variables and examined for their influences on the material properties such as sintered density and microstructure. For more efficient milling operations, an improved two-stage attrition mill was employed and, also a granulation step was introduced to simulate actual pellet fabrication. Co-precipitated

* Corresponding author. Fax: +82-42 868 8868; e-mail: ywlee@nanum.kaeri.re.kr

powder with ammonia and co-precipitated microspheres by internal gelation were also prepared and examined in a similar way to compare pellets fabricated by powders of different fabrication methods.

2. Experimental

2.1. Powder preparation

Three different routes have been separately taken for the powder preparation: (1) dry mixing and milling of the oxide constituents, (2) co-precipitation of mixed solutions by use of ammonia with the composition of $ZrO_2 - 17 \text{ at.}\% YO_{1.5} - 4 \text{ at.}\% ErO_{1.5} - 9 \text{ at.}\% CeO_2$ and (3) co-precipitation in the form of microspheres by internal gelation with the composition of $ZrO_2 - 10 \text{ at.}\% YO_{1.5} - 4 \text{ at.}\% ErO_{1.5} - 9 \text{ at.}\% CeO_2$. Among the three different powder preparation routes, the composition of powder mixtures was varied only for the mixture prepared by dry milling, with the amount of yttrium oxide: $ZrO_2 - n \text{ at.}\% YO_{1.5} - 7 \text{ at.}\% ErO_{1.5} - 15 \text{ at.}\% CeO_2$ with $n = 5, 10$ and 15 . These three different compositions of powder mixtures were separately prepared and compared in order to see the effect of amount of Y_2O_3 on the sintering behaviour of the compositions.

2.1.1. Description of the two-stage attrition mill utilised

A conventional attrition mill is mostly operated in wet milling media and can be continuous. A dry attrition mill [5–7], which is usually considered batch type, is operated by revolution of vertical shaft with paddles at the center of the mill jar containing milling media (steel or ceramic balls). On revolution of the shaft, the movement of the milling media, which take the powder being milled, is such that it flows down rapidly around the shaft to the bottom in helical motion and upwards near the inner surface of the mill jar. Consequently, the time taken for the powder being milled to arrive at the bottom is short and large amount of the powder remains and tends to stick on the bottom and the surface, and even at the lower edge in the mill jar.

A two-stage attrition mill was developed to improve the conventional batch type dry attrition mill, in view of the efficiency and the problems often encountered during operation: powder sticking onto the inner wall, agglomerating in the edge of lower part of the mill jar and rapid fall-down of the powder. The mill jar where the powder milling takes place is separated by a steel grid into upper and lower parts and the shaft has various kinds of paddles with specially designed shapes for each part (Fig. 1). The shapes and arrangement of the paddles are so combined that when the shaft turns the milling media (ceramic balls) move effectively enough for the powders being milled to stay for longer duration in the milling media. Once the powder is passed through

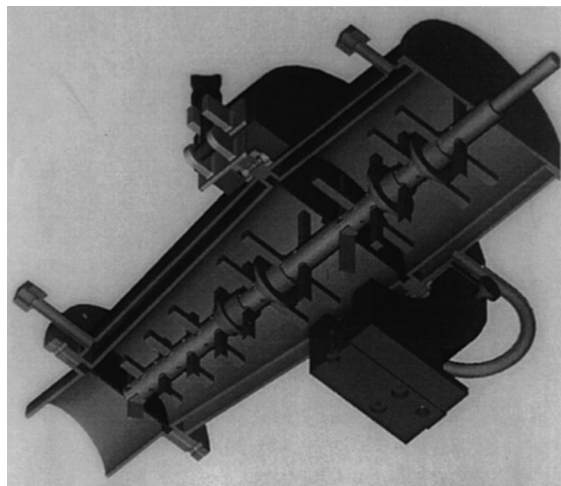


Fig. 1. Inner structure of the two-stage attrition mill showing its shaft with paddles (total volume of mill: 1.5 dm^3 , volume of ball media: 1 dm^3 , used in the experiment).

the upper stage, the powder will then be continuously milled in the lower stage, where the milling operation will be refined with a different size of milling media and the shape of the paddles. Thus, by adjusting the sizes of milling media in each stage and by choosing different shapes of the paddles, the milling operation can be optimised. This improvement gives much easier handling of the materials especially when nuclear materials are concerned with respect to undesirable mixing of the different fissile contents from a lot to another and complexity in handling for the works in confinements.

2.1.2. Preparation of powder mixtures by dry milling

Three different compositions of powder mixture ($ZrO_2 - n \text{ at.}\% YO_{1.5} - 7 \text{ at.}\% ErO_{1.5} - 15 \text{ at.}\% CeO_2$ with $n = 5, 10$ and 15) were prepared using commercially available chemical products: ZrO_2 and CeO_2 powders with more than 99% of purity purchased from Fluka™ and Y_2O_3 and Er_2O_3 powders with more than 99.9% of purity purchased from Cerac™. The mean particle sizes of the starting materials are 3.6, 9.3, 9.6 and $27.7 \mu\text{m}$ for ZrO_2 , Y_2O_3 , Er_2O_3 and CeO_2 , respectively. The weighed amounts of each oxide powder were mixed in a Turbula™ mixer for 4 h and then milled with the improved two-stage attrition mill. The specially-designed shaft of the attrition mill turned at about 200 rpm, which gave the total length of time of about 2–4 min for one passage of the powder through the mill depending on the powder property with the number of passages. The milled powder samples were subsequently granulated by precompacting with pressure in the range of 100 and 500 MPa and forced-sieving through 1 mm openings in order to simulate actual pellet fabrication, as well as for the milled powder samples to be flowable.

2.1.3. Preparation of co-precipitated powder

All solutions were prepared by mixing a nitrate solution of each element (Zr, Y, Er, or Ce) composing the final product. The starting materials were: $\text{ZrO}(\text{NO}_3)_2 \cdot 32\% \text{H}_2\text{O}$, purum, FlukaTM, $\text{Y}(\text{NO}_3)_3 \cdot 27\% \text{H}_2\text{O}$, puriss., FlukaTM, $\text{Er}(\text{NO}_3)_3 \cdot 5 \text{H}_2\text{O}$, (>99.9%), AldrichTM and $\text{Ce}(\text{NH}_4)_2(\text{NO}_3)_6$, puriss. p.a., FlukaTM.

Co-precipitation was carried out by adding ammonia (NH_4OH) under strong stirring. The precipitate was filtered on a glass filter type P4 which corresponds to a filter pore size of $(13 \pm 3) \mu\text{m}$ and washed with ultrapure water until a pH-value of 8 was reached. The filtered phase was additionally washed with ethanol. The wet powder was then dried in a heating locker at 390 K for 6 h and milled utilising a RetschTM unit with a zirconia container and balls. A calcination procedure of 6 h at 1070 K followed. The calcined powder was milled again utilising the same mill. The problem of this simple production method was the slow filtration of the hydroxide cake. As an example, for the large 100 gram batches, the whole procedure of filtration and washing took about 2 days using a 17 cm diameter filter.

2.1.4. Preparation of co-precipitated microspheres

Spheres were gelled following the internal gelation process with nitrate solutions as the starting material. The gelation parameters like free acid in the solution, hexamethylenetetramine (HMTA) and urea contents, the gelation time, temperature conditions on the gelation behaviour were investigated in detail. The feed solution was prepared by mixing the nitrate solutions of the different metals according to the desired composition of the final product. Good conditions were found with the following composition: metal concentration 0.6 mol kg^{-1} , HMTA to metal molar ratio of 1.20, urea to metal molar ratio of 0.026, total nitrate to metal molar ratio of 2.75 and free acid to metal molar ratio of 0.18. The gelation temperature was held at 383 K for a sphere size of $700 \mu\text{m}$ and a vibrated nozzle was used for uniform droplets generation at a high throughput. The heat carrier was removed by ActrelTM on belt filters and washing was performed with ammonia in a batch type washing operation in baskets. The microspheres have been dried at 353 K in air under stationary conditions and calcined under flowing gas at different temperatures according to the powder characteristics to be tested for pellet fabrication. The batch size was in the order of a hundred gram. Characterisation of the dried and calcined sphere focused on X-ray diffraction, chemical analysis and technological characterisation with tap density and BET surface area measurements.

2.2. Fabrication of pellet specimens

The milled powder mixture samples were compacted into pellets with a pressure range between 300 and 500

MPa by use of double-acting hydraulic press for the dwell time of 30 s. The die diameter was 11.6 mm and a pellet height of 10 mm was anticipated. Sintering of the pellet specimens was carried out in a tube furnace for 5, 12 and 24 h at 1873 K and for 5 h at 1923 K under flowing air.

2.3. Analyses of milled powder mixtures and pellet specimens

The milled powder mixtures, prepared in different milling conditions, were analysed by using a MasterSizerTM (Malvern, UK) for granulometry and their tap densities were measured following the procedures described in ASTM B-527 using AutotapTM (Quantachrome, Model DA-1, USA) and the pour densities using the AlcanTM flowmeter. Sintered densities were measured by the water immersion method and for the microstructural observation of pellet specimens with an optical microscope, a mixed solution of equal volume of NH_4F and H_2O heated to 383 K was used to reveal the grains and the grain boundaries. Pore size distribution was determined with image analysis software AnalySIS.¹ Average grain size was measured by the linear intercept method. For the phase identification an X-ray diffraction (XRD) unit MXP3A-HF (MacScience, Japan) was used at KAERI, whereas at PSI, XRD phase analysis was performed with a Philips diffractometer PW1720 and the 'PW1877 Automated Powder Diffraction 3.6B' software for interpretation with nickel powder as an internal standard.

3. Results and discussion

3.1. Powder granulometry and densities

The variations of the mean particle size for the three different compositions of powder mixtures as a function of the number of milling passages are shown in Fig. 2. The milling operation usually gives a sufficient homogeneity of powder mixtures accompanied by powder size reduction and, thus the milling of powder to a smaller particle size indirectly indicates a level of the homogeneity of a powder mixture. The mean particle size decreases with the number of mill passages up to 14 times, then it seems to increase (Fig. 2). This implies that with more than 14 mill passes, the powder mixture tends to agglomerate, indicating the segregation of the powder mixture.

Table 1 shows pour and tap densities of $\text{ZrO}_2 - 10 \text{ at.}\% \text{YO}_{1.5} - 7 \text{ at.}\% \text{ErO}_{1.5} - 15 \text{ at.}\% \text{CeO}_2$ powder

¹ Image Analysis Software AnalySIS Version 2.1 of Soft-Imaging GmbH, Germany.

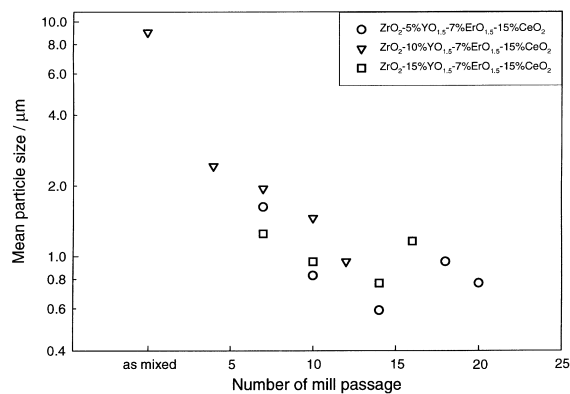


Fig. 2. Variations of mean particle size for three different compositions of powder as a function of the number of mill passages in dry milling powder preparation.

mixtures milled and granulated in different conditions. It shows that these powder densities are nearly independent of the number of mill passages for milled powder but that these densities are varied for the granulated powders with granulation conditions and increased compared with those for milled powder mixtures.

3.2. Green and sintered pellet density relations for various milled powder mixtures

The variations in green density of milled and granulated powder mixtures of three different compositions with the number of mill passages are shown in Fig. 3. The green density decreases with the number of mill passages, indicating that green pellets with granulated smaller particles have more open voids among granulates and that the green density increases with compaction pressure. The influence of the number of mill passages on sintered density is also shown in Fig. 3. for the green pellet specimens of three different compositions compacted with 300 and 500 MPa and sintered at 1873 K for 5 h in air. The sintered density increases with the number of mill passages for each composition, which is inverse to that for the green density. Moreover, for

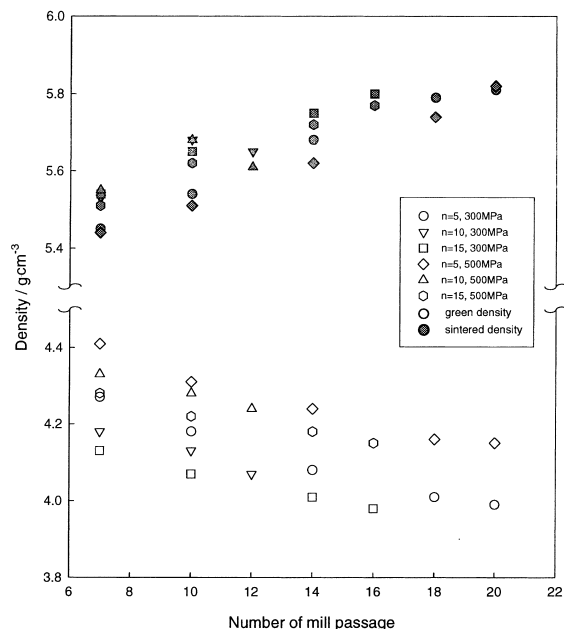


Fig. 3. Variation of green and sintered density of milled and granulated powder mixtures compacted with 300 and 500 MPa and sintered at 1873 K for 5 h in air of three different compositions as a function of number of mill passage in dry milling powder (n denotes in the legend the values in the composition $ZrO_2 - n$ at.% $YO_{1.5} - 7$ at.% $ErO_{1.5} - 15$ at.% CeO_2 preparation and the values in MPa denote the compaction pressure).

two different levels of compaction pressures (300 and 500 MPa), the pellet specimens achieve slightly higher density with lower compaction pressures. It is also worthwhile to note that, for the different contents of Y_2O_3 , pellet specimens sinter to a larger extent with higher content of Y_2O_3 than that with less Y_2O_3 .

The effect of sintering time on the sintered density for different compaction pressures is shown in Fig. 4. for the powder mixture of $ZrO_2 - 10$ at.% $YO_{1.5} - 7$ at.% $ErO_{1.5} - 15$ at.% CeO_2 . Sintering time has much greater effect on sintered density than compaction pressure (300 and 500 MPa) and sintering temperature (1873 and 1923 K).

Table 1

Variations of pour and tap densities as a function of number of mill passage for the composition of $ZrO_2 - 10$ at.% $YO_{1.5} - 7$ at.% $ErO_{1.5} - 15$ at.% CeO_2 by dry milling and granulation (standard deviation: ≤ 0.05 g cm $^{-3}$)

Number of passage through mill jar	Pour density (g cm $^{-3}$)	Tap density (g cm $^{-3}$)
As mixed	1.43	2.22
4 passages	1.54	2.20
7 passages	1.60	2.22
10 passages	1.60	2.20
12 passages	1.60	2.20
Granulated; 500 MPa, 75 rpm	2.17	2.58
Granulated; 500 MPa, 50 rpm	2.10	2.67
Granulated; 300 MPa, 135 rpm	2.04	2.58

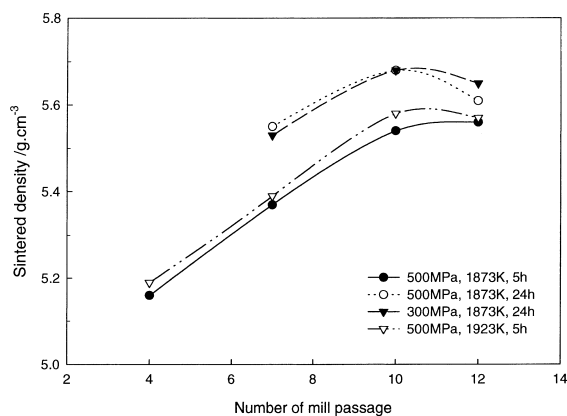


Fig. 4. Effect of sintering time and compaction pressure on the sintered density for the powder mixture of the composition $\text{ZrO}_2 - 10 \text{ at.}\% \text{YO}_{1.5} - 7 \text{ at.}\% \text{ErO}_{1.5} - 15 \text{ at.}\% \text{CeO}_2$ sintered at 1873 K in air.

This effect becomes less when the number of mill passages increases (See Table 2).

3.3. Observation of microstructures and ceramographic examination

The pore structure variations of the pellet specimens with a composition $\text{ZrO}_2 - 10 \text{ at.}\% \text{YO}_{1.5} - 7 \text{ at.}\% \text{ErO}_{1.5} - 15 \text{ at.}\% \text{CeO}_2$ are shown in the micrographs given in Fig. 5. They were obtained under different sintering conditions: pellet specimens in (a) and (b) with the powder mixture milled once, compacted with 100 MPa and sintered for 4 h in air at 1673 and 1773 K, respectively, and, (c) and (d) are those specimens compacted with 200 MPa and sintered at 1873 K for 12 h in air

from the powder mixtures milled with 3 and 4 mill passages, respectively. This illustrates clearly how sintering temperature and time affect the pore morphology and distribution. The densification of the pellet specimens seems to be as follows: at higher temperatures, as in (c) and (d), larger pores disappear compared with (a) and (b), suggesting the elimination of large pores, which contribute strongly to the densification. This effect is confirmed by the densities determined for the different products.

The result of different powder characteristics used for granulation and sintering is shown in the pore microstructure of sintered pellets (Fig. 6). The two products result in the same apparent density of 91% TD after compacting with a pressure of 300 MPa and sintering at 1873 K for 10 h in air. For the pellets starting from individual powders with 15 passes through the attrition mill a homogeneous pore distribution, shown in Fig. 6 top, is found. Whereas the ceramographic picture of the pellet from coprecipitated powder with only 10 passes (Fig. 6 bottom) shows less than half the area of pores (Table 3) with a smaller equivalent circular diameter (ECD) but also some very large pores. The difference can be explained with the higher sinter activity indicated by the high value of the measured surface area and the incomplete mixing of the coprecipitated powder in the mill [8].

For the grain growth, however, the sintering time does not seem to affect to a large extent the grain size in the range of the sintered density obtained in the experiment which is nearly constant at 1873 K and about 10 μm in average, as shown in Fig. 7(a) and (b), in contrast with the sintered density which is influenced mostly by sintering time among the parameters considered as shown previously in Fig. 4.

Table 2
Characteristics of powder and granulate

Parameter	Mixed powder, prepared at KAERI	Mixed powder, prepared at PSI	Co-precipitated powder, dried spheres, prepared at PSI
BET-surface area/ $\text{m}^2 \text{g}^{-1}$	Not determined	7.4	180.0
<i>Calcined and milled powder</i>			
Composition	$(\text{Zr}_{0.68}\text{Y}_{0.10}\text{Er}_{0.07}\text{Ce}_{0.15})\text{O}_2$	$(\text{Zr}_{0.70}\text{Y}_{0.17}\text{Er}_{0.04}\text{Ce}_{0.09})\text{O}_2$	$(\text{Zr}_{0.68}\text{Y}_{0.10}\text{Er}_{0.07}\text{Ce}_{0.15})\text{O}_2$
Calcined (temperature/time)	—	—	823 K/7 h
Passes in attrition mill	10 times	15 times	10 times
Flowability	Not flowable	Not flowable	Not flowable
Pour density (g cm^{-3})	1.60	1.42	1.32
Tap density (g cm^{-3})	2.20	1.92	1.89
BET-surface area ($\text{m}^2 \text{g}^{-1}$)	Not determined	8.5	53.3
Particle size (μm)	1.46	Not determined	Not determined
<i>Granulated powder</i>			
Flowability	Good	Good	Good
Pour density (g cm^{-3})	2.04	1.78	1.56
Tap density (g cm^{-3})	2.58	2.12	1.84

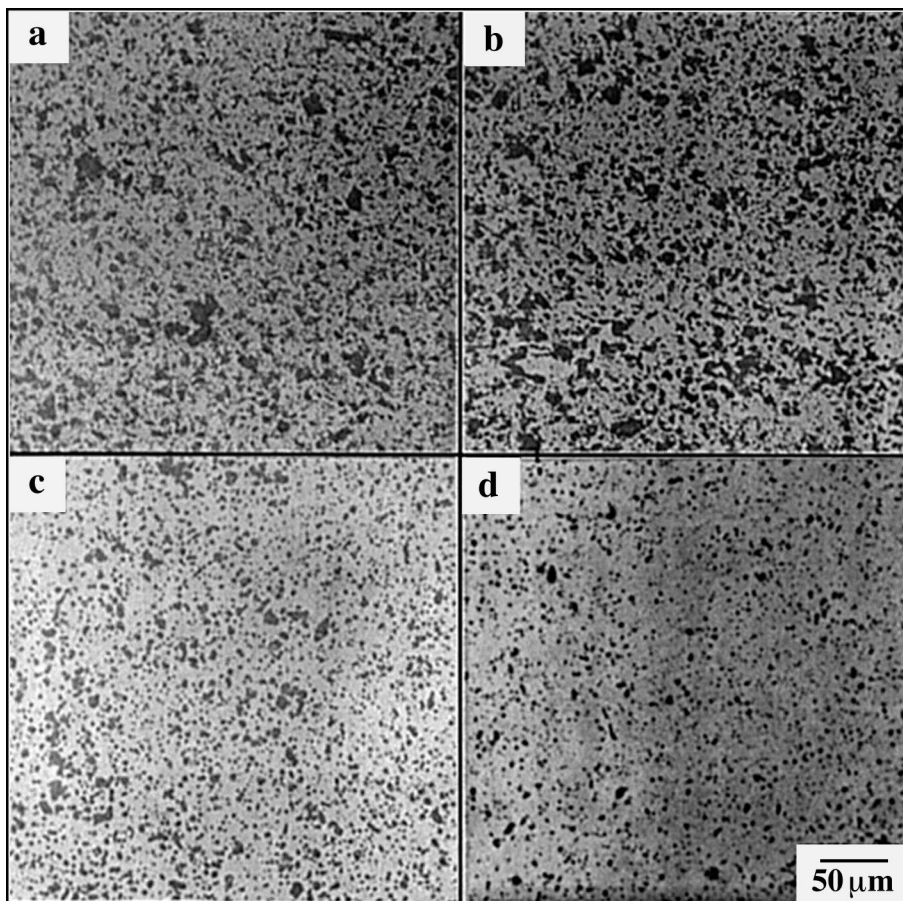


Fig. 5. Pore micrograph for the sintered pellet specimens in the composition $\text{ZrO}_2 - 10 \text{ at.}\% \text{YO}_{1.5} - 7 \text{ at.}\% \text{ErO}_{1.5} - 15 \text{ at.}\% \text{CeO}_2$ obtained from different conditions: (a) compacted with 100 MPa and sintered at 1673 K; (b) compacted with 100 MPa and sintered at 1773 K; (c) milled with three passages, compacted with 200 MPa and sintered at 1873 K for 5 h and (d) milled with four passages, compacted with 200 MPa and sintered at 1873 K for 5 h.

3.4. Identification of phase by X-ray diffractometry

The XRD patterns for coprecipitated powder does not reveal any crystal structure whereas the powder mixture (Fig. 8) gives independent patterns for the different oxides used, i.e., monoclinic ZrO_2 and cubic Y_2O_3 , Er_2O_3 and CeO_2 . Calcination of the coprecipitated powder transforms the amorphous material between 773 and 1273 K in a tetragonal phase with very small crystallites and the XRD patterns for the pellet specimens sintered at 1673, 1773 and 1873 K, respectively, show the pattern of a homogeneous single cubic phase of stabilised ZrO_2 (Fig. 8).

4. Conclusion

This study covered the preparation of simulated ZrO_2 -based IMF by a dry powder milling method.

Powder milling and sintering parameters which can affect the microstructure and density of product were taken as variables. Different methods have been applied for the powder preparation. In addition to powder mixing, nitrate solutions have been coprecipitated to bulk gel and to microspheres by the internal gelation process. From the experiment, the following conclusions are pointed out:

The dry attrition mill specially-designed for homogeneous products and improved for more suitable use with fine powder can be successfully employed for dry milling of ZrO_2 -based inert matrix fuel materials.

- In the milling operation of the materials, the number of mill passages for the maximum efficiency is about 12–15 times, after which the milling results in the agglomeration of powder and the segregation of mixtures.
- The green density of compacts of three compositions decreases and the sintered density increases with the

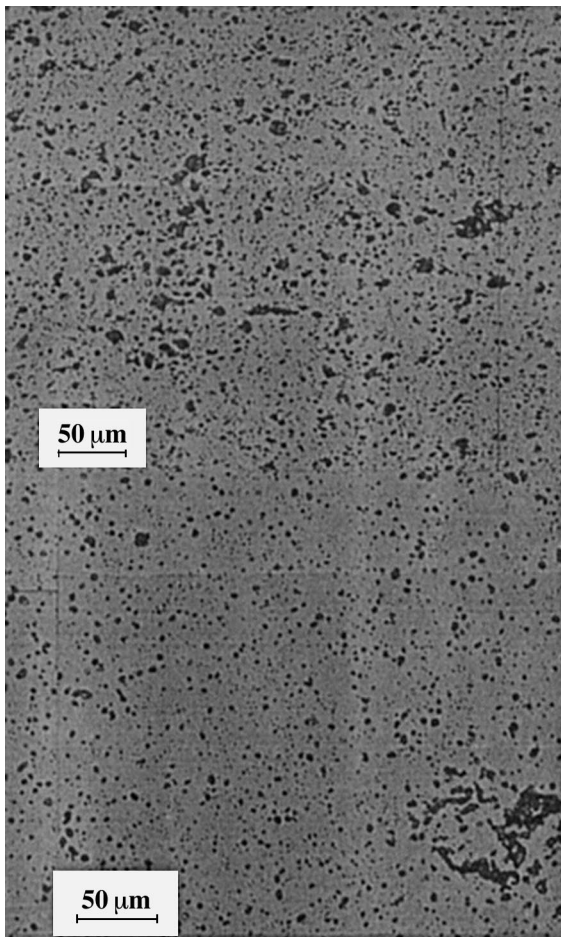


Fig. 6. Pore micrograph of the sintered pellet specimens in the composition $\text{ZrO}_2 - 10 \text{ at.}\% \text{YO}_{1.5} - 7 \text{ at.}\% \text{ErO}_{1.5} - 15 \text{ at.}\% \text{CeO}_2$ compacted with 300 MPa and sintered at 1873 K for 10 h in air (top: powder mixture with 15 passages and, bottom: coprecipitated powder milled with 10 passages).

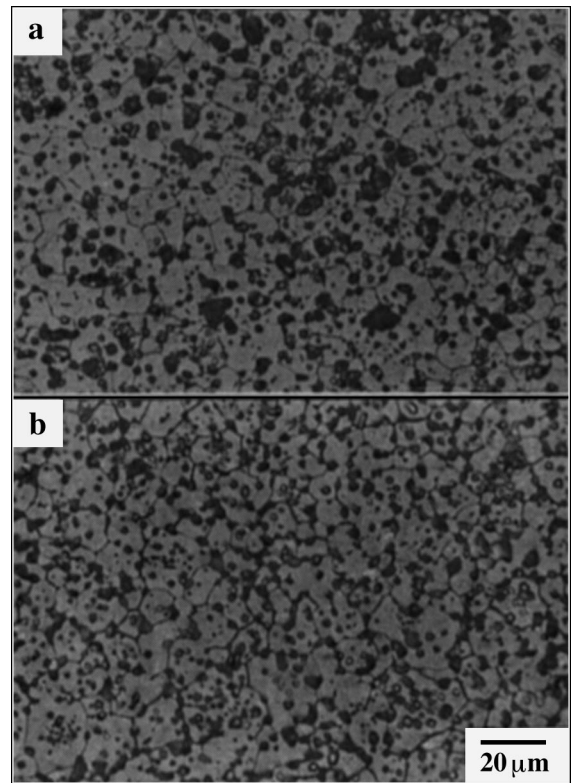


Fig. 7. Grain structures of the sintered pellet specimens in the composition $\text{ZrO}_2 - 10 \text{ at.}\% \text{YO}_{1.5} - 7 \text{ at.}\% \text{ErO}_{1.5} - 15 \text{ at.}\% \text{CeO}_2$ obtained from different conditions: (a) milled with seven passages, compacted with 500 MPa and sintered at 1873 K for 24 h in air and (b) milled with 10 passages, compacted with 300 MPa and sintered at 1873 K for 5 h in air.

Table 3
Characteristics of pellet specimens

Parameter	Mixed powder, prepared at KAERI (7IM-T002)	Mixed powder, prepared at PSI (7IM-T007)	Coprecipitated powder, prepared at PSI (7IM-T017)
Composition	$(\text{Zr}_{0.68}\text{Y}_{0.10}\text{Er}_{0.07}\text{Ce}_{0.15})\text{O}_2$	$(\text{Zr}_{0.70}\text{Y}_{0.17}\text{Er}_{0.04}\text{Ce}_{0.09})\text{O}_2$	$(\text{Zr}_{0.68}\text{Y}_{0.10}\text{Er}_{0.07}\text{Ce}_{0.15})\text{O}_2$
Green density (g cm^{-3})	4.16	3.57	3.26
Sintered density (g cm^{-3}) 1873 K/10h/air	5.68 (88.9%TD)	5.55 (90.1%TD)	5.91 (92.4%TD)
<i>Ceramography</i>			
Pore structure	Homogeneous	Homogeneous	Few very large pores
Pore size (ECD) (μm)	10 ± 5	3.6 ± 1	3.3 ± 1
Pore fraction (%)	15 ± 5	15 ± 5	7 ± 5
Grain size (μm)	17	14	17
<i>XRD</i>			
Lattice parameter (nm)	Cubic, single phase 0.5187	Cubic, single phase 0.5176	Cubic, single phase 0.5185
Th. density (TD) (g cm^{-3})	6.40	6.16	6.40

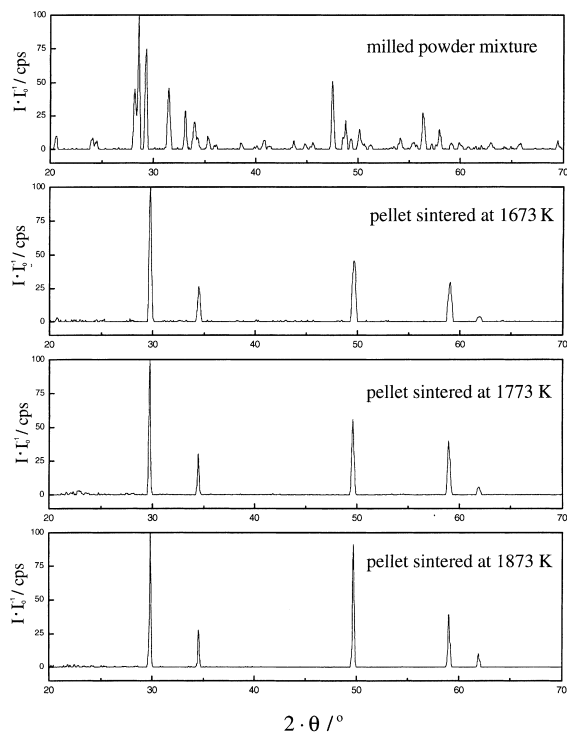


Fig. 8. XRD patterns for the powder mixture before sintering and sintered with different temperatures (sintering time: 5 h).

number of mill passages. The green density increases as compaction pressure increases. However, sintered density decreases slightly as compaction pressure increases.

- The effect of sintering time on densification is much larger than that of temperature and, for the three different compositions, the higher the content of Y_2O_3 in the powder mixture, the higher the obtained sintered density. Meanwhile, the grain size obtained by

sintering at 1873 K is about 10 μm , and is nearly constant irrespective of sintering time.

- Co-precipitated powder influences the pore structure of the pellets and the formation of single phase cubic stabilised zirconia was found independent of composition and powder quality.

Acknowledgements

The authors would like to thank to T. Xie and S. Lutique for their evaluation of sphere fabrication conditions and M. Streit, F. Wyss and T. Graber for their effort in the characterisation of this new materials. This work has been carried out partly under the Nuclear R&D Program by the Ministry of Science and Technology in Korea.

References

- [1] J.M. Paratte, R. Chawla, *Ann. Nucl. Energy* 22 (1995) 471.
- [2] C. Degueldre, U. Kasemeyer, F. Botta, G. Ledergerber, *Mater. Res. Soc. Symp. Proc.* 412 (1995) 15.
- [3] G. Ledergerber, C. Degueldre, U. Kasemeyer, A. Stanculescu, J.M. Paratte, R. Chawla, Status of the inert matrix fuel program at PSI, in: *Proceedings of the Second Seminar on the New Fuel Technology Toward the 21st Century*, Korea Atomic Energy Research Institute, Taejon, Korea, 25–26 November 1997, pp. 23–36.
- [4] U. Kasemeyer, R. Chawla, P. Grimm, J.M. Paratte, *Nucl. Technol.* 122 (1998) 52.
- [5] D.A. Stanley et al., *J. Am. Ceram. Soc.* 53 (1974) 813.
- [6] R. Goodson, L. Sheehan, *Modern Dev. in Powder Metall.* 17 (1985) 165.
- [7] H.M. Mcleod, J. Yares, *Nucl. Tech.* 102 (1993) 3.
- [8] G. Ledergerber, W. Dörr, R.W. Stratton, M. Peehs Uranium oxide pellets from microspheres sintered under NIKUSI conditions, *Proceedings of the European Nuclear Conference (ECN-90) Lyon*, September 1990, pp. 23–28.